Direction-of-Arrival Estimation of Mixed Coherent and Uncorrelated Signals

Saidur R. Pavel, *Student Member, IEEE*, and Yimin D. Zhang, *Fellow, IEEE*

***Abstract*—This letter develops a new direction-of-arrival (DOA) estimation method for mixed coherent and uncorrelated signals through the reconstruction of a set of Toeplitz matrices. More specifically, Toeplitz matrices are formed by utilizing the rows and columns of the covariance matrix, and their average is used by subspace-based algorithms to effectively estimate the signal DOAs. Compared to existing methods, the proposed approach provides a high number of degrees of freedom and requires a low computation complexity.**

***Index Terms*—Direction of arrival estimation, Toeplitz matrix reconstruction, mixed coherent and uncorrelated signals.**

I. Introduction

DIRECTION-of-arrival (DOA) estimation is an important area of research in array signal processing applied to radar, sonar, and wireless communications [1]–[6]. Among the various methods developed for DOA estimation, subspace-based approaches, such as the MUltiple SIgnal Classification (MUSIC) [7] and Estimation of Signal Parameters via Rotational Invariance Techniques (ESPRIT) [8], are popularly exploited due to their capability to achieve high-resolution DOA estimation with a low complexity. Leveraging the eigenstructure of the covariance matrix of the sensor array output, these methods are most effective when all the impinging signals are uncorrelated and, as a result, the yielding covariance matrix is full rank. However, in real-world applications, we often encounter coherent signals that may arise due to phenomena such as multipath propagation in wireless communications as well as low-angle reflection in radar sensing [9], [10]. In such cases, the obtained covariance matrix becomes rank-deficient and, as a result, direct application of the subspace-based DOA estimation methods becomes infeasible.

Several methods have been developed to decorrelate coherent signals and restore the rank of the covariance matrix. Among them, the well-known spatial smoothing method partitions the array into multiple overlapping subarrays and averages the covariance matrices over these subarrays to construct a full-rank covariance matrix [11]. The main drawback of this approach is that the number of degrees of freedom (DOFs) is limited to approximately half of the number of sensors. In [12], the forward-backward spatial smoothing technique was developed to increase the number of DOFs to approximately two-thirds of the number of sensors. By forming a Toeplitz coveriance matrix, a computationally efficient method was developed in [13] to estimate the signal DOAs without performing spatial smoothing. However, similar to the spatial smoothing, the number of resolvable signals remains approximately half of the number of sensors. This method is further improved by increasing the dimension of the signal subspace in [14] by utilizing both forward and backward vectors lying in the signal subspace. Two methods are developed based on this concept, namely, the eigenvector method (EVM) and the correlation vector method (CVM), to obtain the forward and backward vectors. These approaches achieve a similar number of DOFs as the forward-backward spatial smoothing. This decorrelation concept is extended to two-dimensional sparse arrays in [15], where the four-dimensional covariance tensor is decorrelated by exploiting a particular slice from the covariance tensor and rearranging it in a Toeplitz fashion. In [16], a DOA estimation method based on maximum likelihood (ML) estimation is developed, exhibiting robust performance even in the presence of coherent signals. This method is further extended to sparse arrays [17], showing the capability of detecting more sources than the number of sensors in a sparse array.

Detecting a mixture of coherent and uncorrelated signals can be even more challenging. Such problem is considered for uniform linear arrays (ULAs) in [18] by first detecting the uncorrelated sources using subspace-based algorithms, such as MUSIC, and the symmetric array configuration is exploited to remove their contribution from the data covariance matrix, leaving only the coherent components. This coherent covariance matrix is then decorrelated by constructing a Toeplitz matrix [13], enabling the estimation of the coherent sources. In [19], DOA estimation of mixed coherent and uncorrelated signals is addressed within a multiple-input multiple-output (MIMO) radar framework. In this approach, both the transmit and receive arrays are sparse ULAs forming a coprime sum coarray. The DOAs of the coherent signals are estimated using complex Bayesian compressive sensing techniques [20].

In this letter, we develop a new DOA estimation method for mixed coherent and uncorrelated signals by exploiting multiple rows and columns of the rank-deficient covariance matrix to construct a set of Toeplitz matrices. The average of these matrices exhibits a Toeplitz-Hermitian property and recovers the full rank of the covariance matrix. The resulting decorrelated covariance matrix is then utilized to detect mixed coherent and uncorrelated sources using subspace-based DOA estimation methods. The proposed methods can resolve more sources than spatial smoothing [11], Toeplitz reconstruction-based methods [13], and their associated forward-backward

This work was supported in part by the National Science Foundation (NSF) under Grant ECCS-2236023 and in part by the Air Force Office of Scientific Research (AFOSR) under Grant FA9550-23-1-0255.

The authors are with the Department of Electrical and Computer Engineering, Temple University, Philadelphia, PA 19122, USA (emails: pavel.saidur@temple.edu, ydzhang@temple.edu).

variances [12], [14]. This method also provides comparable performance to the ML-based approach [16] but with significantly lower computational costs.

Notations: We use bold lower-case (upper-case) letters to describe vectors (matrices). Specifically, $\boldsymbol{I}_L$ represents the identity matrix of size $L \times L$, and $\boldsymbol{0}_L$ and $\boldsymbol{1}_L$ denote $L \times 1$ vectors consisting of all zero elements and all one elements, respectively. $(\cdot)^{\mathrm{T}}$, $(\cdot)^*$ and $(\cdot)^{\mathrm{H}}$ respectively indicate the transpose, conjugate, and conjugate transpose (Hermitian) of a matrix or a vector. triu$(\cdot)$ denotes the upper triangular elements of a matrix, whereas tril$(\cdot)$ denotes the lower triangular elements with the diagonal elements excluded. Furthermore, symbols $\circ$, $\oslash$, $(\cdot)^{\circ m}$ denote the element-wise (Hadamard) product, division, and the mth power, respectively. The symbol $j = \sqrt{-1}$ represents the unit imaginary number and $\lfloor \cdot \rfloor$ denotes the floor operation. Finally, $\mathbb{E}(\cdot)$ denotes the statistical expectation, diag$(\cdot)$ and bdiag$(\cdot)$ respectively represent the construction of a diagonal matrix and a block-diagonal matrix, and $\delta_{m,k}$ denotes the Kronecker delta function.

II. Signal Model

Consider a ULA consisting of M omnidirectional sensors, and P far-field narrowband signals impinge on the array from DOAs $\boldsymbol{\theta} = [\theta_1, \theta_2, \cdots, \theta_P]^{\mathrm{T}}$. Among them, the first L signals exhibit mutual coherence, while the remaining $P - L$ signals are uncorrelated with each other and with the coherent group. The signal vector received at time t can be expressed as

$$\begin{aligned}\boldsymbol{x}(t) &= s_1(t)\sum_{i=1}^{L}\alpha_i\boldsymbol{a}(\theta_i) + \sum_{i=L+1}^{P} s_i(t)\boldsymbol{a}(\theta_i) + \boldsymbol{n}(t) \\ &= \boldsymbol{A}_c\boldsymbol{s}_c(t) + \boldsymbol{A}_u\boldsymbol{s}_u(t) + \boldsymbol{n}(t) = \boldsymbol{A}\boldsymbol{s}(t) + \boldsymbol{n}(t),\end{aligned} \tag{1}$$

where $\boldsymbol{a}(\theta_i) = [1, e^{-j\frac{2\pi}{\lambda}d\sin\theta_i}, \cdots, e^{-j\frac{2\pi}{\lambda}(M-1)d\sin\theta_i}]^{\mathrm{T}} \in \mathbb{C}^{M\times 1}$ is the steering vector associated with DOA θ_i, $\boldsymbol{A} = [\boldsymbol{a}(\theta_1), \cdots, \boldsymbol{a}(\theta_P)] \in \mathbb{C}^{M\times P}$ is the array manifold matrix with $\boldsymbol{A}_c = [\boldsymbol{a}(\theta_1), \cdots, \boldsymbol{a}(\theta_L)]$ and $\boldsymbol{A}_u = [\boldsymbol{a}(\theta_{L+1}), \cdots, \boldsymbol{a}(\theta_P)]$ respectively representing the array manifold matrices for the coherent and uncorrelated sources, $\boldsymbol{s}(t) = [s_1(t), s_2(t), \cdots, s_P(t)]^{\mathrm{T}} \in \mathbb{C}^{P\times 1}$ is the signal waveform vector, and $\boldsymbol{n}(t) \sim \mathcal{CN}(\boldsymbol{0}, \sigma_n^2\boldsymbol{I}_M)$ is the additive white Gaussian noise vector. The waveforms of the coherent signals are identical to the reference signal $s_1(t)$ up to a scalar coefficient α_i, i.e., $s_i(t) = \alpha_i s_1(t),\ \text{for } 1 \le i \le L$.

The covariance matrix of the received signal vector $\boldsymbol{x}(t)$ can be expressed as

$$\begin{aligned}\boldsymbol{R} &= \mathbb{E}[\boldsymbol{x}(t)\boldsymbol{x}^{\mathrm{H}}(t)] = \boldsymbol{A}\boldsymbol{R}_s\boldsymbol{A}^{\mathrm{H}} + \sigma_n^2\boldsymbol{I}_M \\ &= \boldsymbol{A}_c\boldsymbol{R}_c\boldsymbol{A}_c^{\mathrm{H}} + \boldsymbol{A}_u\boldsymbol{R}_u\boldsymbol{A}_u^{\mathrm{H}} + \sigma_n^2\boldsymbol{I}_M,\end{aligned} \tag{2}$$

where $\boldsymbol{R}_c$ and $\boldsymbol{R}_u$ are the source covariance matrices for coherent and uncorrelated signals, respectively, and $\boldsymbol{R}_s = \text{bdiag}(\boldsymbol{R}_c, \boldsymbol{R}_u)$ represents the source covariance matrix for the mixed signals. Due to the correlation assumption, the source covariance matrices $\boldsymbol{R}_c$ and $\boldsymbol{R}_u$ can be expressed as

$$\boldsymbol{R}_c = \sigma_1^2\boldsymbol{\alpha}\boldsymbol{\alpha}^{\mathrm{H}} \tag{3}$$

and

$$\boldsymbol{R}_u = \text{diag}\left([\sigma_{L+1}^2, \cdots, \sigma_P^2]\right), \tag{4}$$

where σ_i^2 is the signal power of the ith signal and $\boldsymbol{\alpha} = [\alpha_1, \alpha_2, \cdots, \alpha_L]^{\mathrm{T}}$ denotes the complex attenuation vector for the coherent signals. The (m,k)th element of $\boldsymbol{R}$ is given as

$$\begin{aligned}R(m,k) =& \mathbb{E}\left\{\left[s_1(t)\sum_{i'=1}^{L}\alpha_{i'}a_m(\theta_{i'}) + \sum_{i'=L+1}^{P} s_{i'}(t)a_m(\theta_{i'})\right]\right. \\ &\left.\cdot\left[s_1^*(t)\sum_{i=1}^{L}\alpha_i^*a_k^*(\theta_i) + \sum_{i=L+1}^{P} s_i^*(t)a_k^*(\theta_i)\right]\right\} \\ &+ \sigma_n^2\delta_{m,k}\end{aligned} \tag{5}$$

for $m, k \in [0, 1, \cdots, M-1]$, where $a_m(\theta)$ denotes the mth element of the steering vector $\boldsymbol{a}(\theta)$. Considering that

$$\mathbb{E}[s_i(t)s_{i'}^*(t)] = \begin{cases}\sigma_1^2, & i = i' = 1, \\ \sigma_i^2, & i = i' \ne 1, \\ 0, & i \ne i',\end{cases} \tag{6}$$

we have

$$\begin{aligned}R(m,k) &= \sigma_1^2\sum_{i'=1}^{L}\alpha_{i'}a_m(\theta_{i'})\sum_{i=1}^{L}\alpha_i^*a_k^*(\theta_i) \\ &\quad + \sum_{i=L+1}^{P}\sigma_i^2a_m(\theta_i)a_k^*(\theta_i) + \sigma_n^2\delta_{m,k} \\ &= \sum_{i=1}^{P} d_{m,i}e^{j\frac{2\pi}{\lambda}dk\sin\theta_i} + \sigma_n^2\delta_{m,k},\end{aligned} \tag{7}$$

where

$$d_{m,i} = \begin{cases}\sigma_1^2\alpha_i^*\sum_{i'=1}^{L}\alpha_{i'}e^{-j\frac{2\pi}{\lambda}dm\sin\theta_{i'}}, & i = 1, 2, \cdots, L, \\ \sigma_i^2e^{-j\frac{2\pi}{\lambda}dm\sin\theta_i}, & i = L+1, \cdots, P.\end{cases} \tag{8}$$

III. Decorrelation of the Covariance Matrix

Due to the presence of cross-correlations between the coherent sources, as evident from Eq. (7), the covariance matrix $\boldsymbol{R}$ exhibits a rank deficiency problem and loses its Toeplitz structure. As a result, applying subspace-based methods directly to $\boldsymbol{R}$ cannot resolve the coherent sources. To address this issue, we develop an effective decorrelation technique to decorrelate the covariance matrix and recover its full rank.

Consider a vector $\boldsymbol{r}_m = [r_m(-(M-1)), \cdots, r_m(M-1)]^{\mathrm{T}}$, whose elements are arranged from the elements in the mth row and the mth column of the covariance matrix $\boldsymbol{R}$, i.e.,

$$\begin{aligned}\boldsymbol{r}_m = &\left[\boldsymbol{0}_m^{\mathrm{T}}\ (\boldsymbol{R}^{\mathrm{T}}(m\!:\!M-1, m)\boldsymbol{J})\ (\boldsymbol{R}(m, m+1\!:\!M-1))\ \boldsymbol{0}_m^{\mathrm{T}}\right]^{\mathrm{T}} \\ &\in \mathbb{C}^{2M-1},\end{aligned} \tag{9}$$

where $\boldsymbol{J}$ is an exchange matrix containing ones in the antidiagonal and zeros elsewhere. Such vectors are arranged in the following way to obtain a Toeplitz matrix,

$$\begin{aligned}\tilde{\boldsymbol{R}}(m) &= \begin{bmatrix} r_m(0) & r_m(1) & \cdots & r_m(M-1) \\ r_m(-1) & r_m(0) & \cdots & r_m(M-2) \\ \vdots & \vdots & \ddots & \vdots \\ r_m(1-M) & r_m(2-M) & \cdots & r_m(0)\end{bmatrix} \\ &= \text{triu}(\boldsymbol{A}\boldsymbol{E}^{\circ m}\boldsymbol{D}(m)\boldsymbol{A}^{\mathrm{H}}) + \text{tril}(\boldsymbol{A}(\boldsymbol{E}^{\circ m})^{\mathrm{H}}\boldsymbol{D}^{\mathrm{H}}(m)\boldsymbol{A}^{\mathrm{H}}),\end{aligned} \tag{10}$$

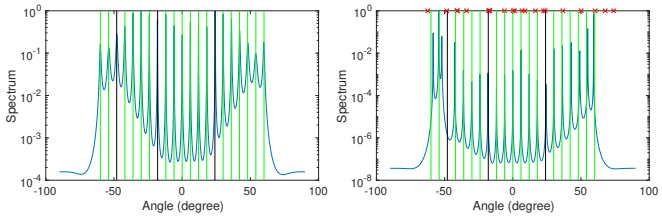

(a) Proposed method. (b) Methods [14] and [16]

Fig. 1: DOA estimation results of 18 uncorrelated and 3 coherent sources. The red crosses represent the estimated DOAs using the method in [14].

where $\boldsymbol{D}(m) = \text{diag}(d_{m,1}, \cdots, d_{m,P})$ and $\boldsymbol{E} = \text{diag}(e^{j\frac{2\pi}{\lambda}d\sin\theta_1}, \cdots, e^{j\frac{2\pi}{\lambda}d\sin\theta_P})$. Another vector $\boldsymbol{c}$ is constructed which contains the occurrence of a correlation corresponding to a particular lag as $\boldsymbol{c}(m) = \left[\boldsymbol{0}_m^{\mathrm{T}}\ \boldsymbol{1}_{2M-2m-1}^{\mathrm{T}}\ \boldsymbol{0}_m^{\mathrm{T}}\right]^{\mathrm{T}}$. We obtain matrix $\boldsymbol{C}(m)$ by arranging the vector $\boldsymbol{c}(m)$ similar to (10). The matrices $\tilde{\boldsymbol{R}}(m)$ for $m = 1, \cdots, (M-1)/2$ are averaged to obtain matrix $\tilde{\boldsymbol{R}}$ as

$$\tilde{\boldsymbol{R}} = \left(\sum_{m=0}^{(M-1)/2} \tilde{\boldsymbol{R}}(m)\right) \oslash \left(\sum_{m=0}^{(M-1)/2} \boldsymbol{C}(m)\right). \tag{11}$$

It is noted that the rank of the noise-free Hermitian Toeplitz matrices $\tilde{\boldsymbol{R}}(m)$ is P, since both $\boldsymbol{A}\boldsymbol{E}^{\circ m}\boldsymbol{D}(m)\boldsymbol{A}^{\mathrm{H}}$ and $\boldsymbol{A}\boldsymbol{E}^{\circ m}\boldsymbol{D}(m)\boldsymbol{A}^{\mathrm{H}}$ are of rank P. Therefore, each of $\tilde{\boldsymbol{R}}(m)$'s has P nonzero eigenvalues. Let $\lambda_p(m)$ be the pth nonzero eigenvalue of $\tilde{\boldsymbol{R}}(m)$ when ordered in ascending order, and let $\tilde{\lambda}_p$ be the pth nonzero eigenvalue of $\sum_{m=0}^{(M-1)/2}\tilde{\boldsymbol{R}}(m)$ when ordered in ascending order. Then, according to Weyl's inequality [21], for these Hermitian matrices, we have

$$\tilde{\lambda}_p \geq \sum_{m=0}^{(M-1)/2} \lambda_p(m) \neq 0. \tag{12}$$

Therefore, the term $\sum_{m=0}^{(M-1)/2}\tilde{\boldsymbol{R}}(m)$, and hence $\tilde{\boldsymbol{R}}$, has at least P nonzero eigenvalues. As a result, $\text{rank}(\tilde{\boldsymbol{R}}) \geq P$, i.e., the Toeplitz Hermitian matrix $\tilde{\boldsymbol{R}}$ recovers the full rank of the covariance matrix. Additionally, since the number of rows in $\boldsymbol{A}$ is M, P can be at most $M-1$ for DOA estimation using subspace-based methods, such as the MUSIC algorithm.

In comparison, the methods developed in [13], [14] decorrelate the covariance matrix by reconstructing a single Toeplitz matrix. [13] utilizes one row of the covariance matrix. As such, the dimension of $\boldsymbol{A}$ is reduced by half, thus only detecting at most $\lfloor (M+1)/2 \rfloor$ sources. [14] utilizes the primary eigenvector corresponding to the largest eigenvalue. It considers the forward vector, which is the primary eigenvector, and a backward vector, which is its flipped and conjugated form. Two Toeplitz matrices are obtained from the forward and backward covariance matrices, and the final decorrelated matrix is the concatenation of these two matrices. This method can detect at most $\lfloor 2M/3 \rfloor$ sources.

IV. Computational Complexity Analysis

The computation of the decorrelated covariance matrix $\tilde{\boldsymbol{R}}$ can be decomposed into the following steps.

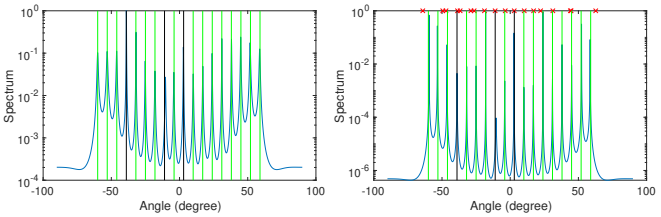

(a) Proposed method (b) Methods [14] and [16]

Fig. 2: DOA estimation results of 15 uncorrelated and 3 coherent sources.

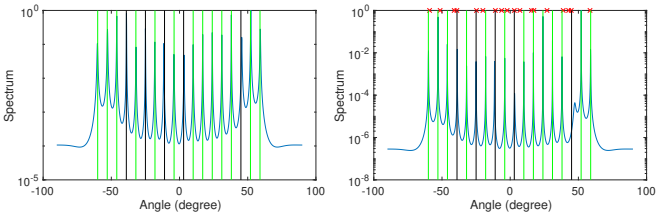

(a) Proposed method (b) Methods [14] and [16]

Fig. 3: DOA estimation results of 13 uncorrelated and 5 coherent sources.

1) Construction of $\boldsymbol{r}_m$: This involves flipping and concatenation of vectors. It does not require any matrix multiplication.
2) Construction of $\tilde{\boldsymbol{R}}(m)$: Reshaping $\boldsymbol{r}_m$ into a Toeplitz matrix $\tilde{\boldsymbol{R}}(m)$ does not require any additional arithmetic operations [22].
3) Construction of $\tilde{\boldsymbol{R}}$: To construct $\tilde{\boldsymbol{R}}$, there are $(M-1)/2$ additions for $\tilde{\boldsymbol{R}}(m)$ and $(M-1)/2$ additions for $\boldsymbol{C}(m)$, and their element-wise division, requiring a complexity of $\mathcal{O}((M-1)^2)$.

Compared to the ML-based approach developed in [16], the proposed approach results in significantly lower computational complexity. In [16], the alternating direction method of multipliers (ADMM) is used to solve a reformulated ML-based estimation problem. The overall algorithm consists of N_o outer loops for the majorization maximization algorithm and N_i inner loops for the 5 update equations in the ADMM algorithm. Each inner loop requires a computational complexity of $\mathcal{O}(M^3)$. Therefore, the total complexity is $\mathcal{O}(N_o N_i M^3)$, which is much higher than that of the proposed algorithm. On the other hand, the ESPRIT-based method with forward-backward vectors (EFBV) requires a lower complexity of $\mathcal{O}(M)$ [14], but the number of DOFs is lower compared to the other two methods.

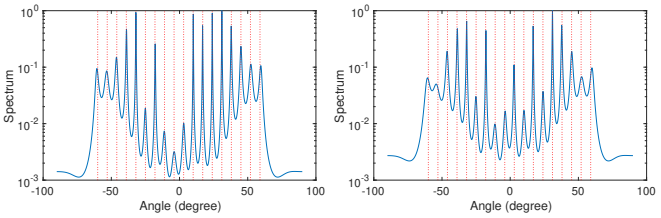

(a) $\rho = 0.3$ (b) $\rho = 0.6$

Fig. 4: DOA estimation results of 18 partially correlated sources.

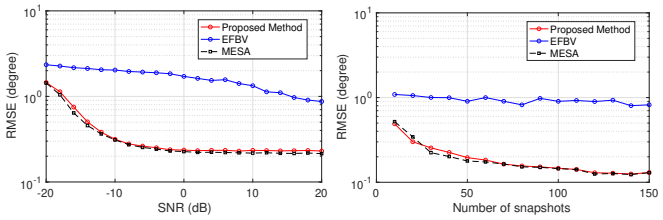

(a) RMSE versus input SNR (b) RMSE versus number of snapshots

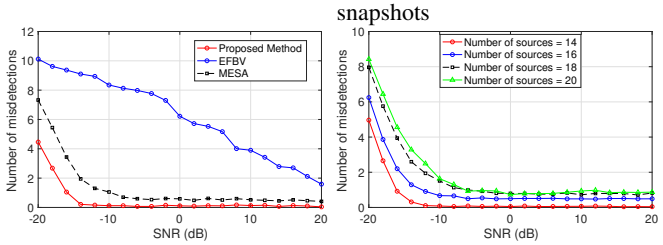

(c) Number of misdetections versus input SNR (d) Number of misdetections of the proposed method for different numbers of sources

Fig. 5: Performance comparison.

V. Simulation Results

We consider a ULA consisting of $M = 25$ sensors to estimate the DOAs in a mixed coherent and uncorrelated signal scenario. We compare the proposed method with the EFBV [14] and the ML-based estimation via sequential ADMM (MESA) [16] in terms of the number of DOFs and DOA estimation performance.

We first consider a high number of sources which is close to the number of sensors. In Fig. 1, 21 sources are considered. Among them, 18 sources are uncorrelated with DOAs $-60°$, $-54°$, $-42°$, $-36°$, $-30°$, $-24°$, $-12°$, $-6°$, $0°$, $6°$, $12°$, $18°$, $30°$, $36°$, $42°$, $48°$, $54°$, $60°$, whereas 3 sources with DOAs $-48°$, $-18°$, $24°$ exhibit mutual coherence. The attenuation factors $\boldsymbol{\alpha}$ are sampled from a complex Gaussian distribution as $\boldsymbol{\alpha} \sim \mathcal{CN}(\mathbf{0}, \boldsymbol{I}_L)$. The input signal-to-noise ratio (SNR) is 10 dB, and 100 snapshots are considered. Fig. 1(a) verifies that the proposed method successfully detects all sources. Note that, the method in [14], which is based on Toeplitz matrix reconstruction using forward and backward vectors, can resolve at most $\lfloor 2M/3 \rfloor = 16$ sources and thus fails to detect the 21 sources as evident from the red crosses depicted in Fig. 1(a). The DOA estimation performance based on [16] is depicted in Fig. 1(b), where one of the coherent sources is undetected. The proposed approach provides a similar number of DOFs and more robust performance compared to [16], particularly when the number of coherent sources is high. We illustrate this by considering 18 mixed sources. As shown in Fig. 2, for 3 coherent sources, both approaches detect all signals successfully. However, as the number of coherent sources increases to 5, as shown in Fig. 3, one of the coherent sources detected using [16] becomes slightly off from its true DOA. EFBV does not perform well in this case either, since the number of sources is higher than the number of DOFs offered by the EFBV.

In addition to the fully coherent case, the proposed model also works for partially correlated sources as well. In Fig. 4, we consider the same 18 sources with correlation coefficients $\rho = 0.3$ and $\rho = 0.6$. The figure clearly shows that the proposed method resolves all partially correlated sources.

Fig. 5(a) compares the root mean-squared error (RMSE) performance with respect to the input SNR for the considered approaches. The RMSE is calculated as

$$\text{RMSE} = \sqrt{\frac{1}{QP}\sum_{q=1}^{Q}\sum_{p=1}^{P}\left(\theta_p - \hat{\theta}_{p,q}\right)^2}, \tag{13}$$

where Q is the number of Monte Carlo trials. In this example, 14 mixed sources are considered, 11 of them being uncorrelated with DOAs $-55°$, $-50°$, $-40°$, $-35°$, $-25°$, $-20°$, $-5°$, $0°$, $10°$, $15°$, and $20°$. The remaining 3 sources are coherent with DOAs $30°$, $45°$, and $44°$. 500 trials are performed for each input SNR to compute the RMSE value. From Fig. 5(a), it is evident that the proposed method provides significantly better performance than [14] and similar performance to [16]. Fig. 5(b) compares the RMSE performance with respect to the number of snapshots. In this case, the input SNR is fixed at 10 dB, and the number of snapshots are varied between 50 and 150. In this case, both the proposed method and the MESA method exhibit similar performance.

To study the robustness, we perform 500 trials as the input SNR varies between -20 dB and 20 dB for a total 14 sources, 11 of which are uncorrelated and the other 3 are mutually coherent. In each trial, the DOAs are randomly generated from a uniform distribution between $-60°$ and $60°$. A DOA is labeled misdetected if the absolute estimation error is larger than $1°$, i.e.,

$$D_{q,p} = \begin{cases} 1, & |\theta_q - \hat{\theta}_{q,p}| \geq 1°, \\ 0, & \text{otherwise}, \end{cases} \tag{14}$$

where $D_{q,p} = 1$ indicates the misdetection of the pth source in the qth trial. Therefore, the number of misdetection per trial is obtained as

$$N_D = \frac{1}{Q}\sum_{q=1}^{Q}\sum_{p=1}^{P} D_{q,p}. \tag{15}$$

Fig. 5(c) depicts a negligible number of misdetection obtained from the proposed model when the input SNR is higher than -10 dB. The number of snapshots is considered to be 500. Fig. 5(d) illustrates the number of misdetections versus the number of sources for the proposed method. The figure shows that, even with 20 sources, the proposed approach detects them effectively, with fewer than 1 average missed detection over 500 trials for input SNRs higher than -8 dB. This confirms that the proposed approach can detect more sources than those in [11], [13], which can detect a maximum of 13 sources, and [12], [14], which can detect up to 16 sources.

VI. Conclusion

In this letter, we addressed the issue of DOA estimation in a mixed coherent and uncorrelated signal scenario. Compared to existing methods based on spatial smoothing and Toeplitz matrix reconstruction, the proposed approach can achieve a higher number of DOFs. Additionally, the proposed approach provides performance similar to the ML-based approach but with significantly lower computational complexity.

REFERENCES

[1] D. H. Johnson, *Array Signal Processing: Concepts and Techniques*. Prentice-Hall, 1993.

[2] H. L. Van Trees, *Optimum Array Processing: Part IV of Detection, Estimation, and Modulation Theory*. Wiley, 2002.

[3] T. E. Tuncer and B. Friedlander, *Classical and Modern Direction-of-Arrival Estimation*. Academic Press, 2009.

[4] M. G. Amin, X. Wang, Y. D. Zhang, F. Ahmad, and E. Aboutanios, "Sparse array and sampling for interference mitigation and DOA estimation in GNSS," *Proc. IEEE*, vol. 104, no. 6, pp. 1302–1317, June 2016.

[5] S. Sun, A. P. Petropulu, and H. V. Poor, "MIMO radar for advanced driver-assistance systems and autonomous driving: Advantages and challenges," *IEEE Signal Process. Mag.*, vol. 37, no. 4, pp. 98–117, 2020.

[6] S. Sun and Y. D. Zhang, "4D automotive radar sensing for autonomous vehicles: A sparsity-oriented approach," *IEEE J. Sel. Topics Signal Process.*, vol. 15, no. 4, pp. 879–891, 2021.

[7] R. Schmidt, "Multiple emitter location and signal parameter estimation," *IEEE Trans. Antennas Propag.*, vol. 34, no. 3, pp. 276–280, 1986.

[8] R. Roy and T. Kailath, "ESPRIT–estimation of signal parameters via rotational invariance techniques," *IEEE Trans. Acoust. Speech signal process.*, vol. 37, no. 7, pp. 984–995, 1989.

[9] T.-J. Shan, M. Wax, and T. Kailath, "On spatial smoothing for direction-of-arrival estimation of coherent signals," *IEEE Trans. Acoust. Speech signal process.*, vol. 33, no. 4, pp. 806–811, 1985.

[10] I. Ziskind and M. Wax, "Maximum likelihood localization of multiple sources by alternating projection," *IEEE Trans. Acoust. Speech signal process.*, vol. 36, no. 10, pp. 1553–1560, 1988.

[11] J. E. Evans, J. R. Johnson, and D. Sun, "Application of advanced signal processing techniques to angle of arrival estimation in ATC navigation and surveillance systems," Massachusetts Institute of Technology, Lincoln Laboratory, Tech. Rep., Cambridge, MA, 1982.

[12] S. U. Pillai and B. H. Kwon, "Forward/backward spatial smoothing techniques for coherent signal identification," *IEEE Trans. Acoust., Speech, Signal Process.*, vol. 37, no. 1, pp. 8–15, 1989.

[13] F.-M. Han and X.-D. Zhang, "An ESPRIT-like algorithm for coherent DOA estimation," *IEEE Antennas Wireless Propagat. Lett.*, vol. 4, pp. 443–446, 2005.

[14] Y.-H. Choi, "ESPRIT-based coherent source localization with forward and backward vectors," *IEEE Trans. Signal Process.*, vol. 58, no. 12, pp. 6416–6420, 2010.

[15] S. R. Pavel, Y. D. Zhang, S. Sun, and A. L. de Almeida, "Tensor reconstruction-based sparse array 2-D DOA estimation of mixed coherent and uncorrelated signals," in *Proc. IEEE Int. Conf. Acoust., Speech, Signal Process. (ICASSP)*, Seoul, Korea, 2024, pp. 12 876–12 880.

[16] Z. Yang and X. Chen, "Maximum likelihood direction-of-arrival estimation via rank-constrained ADMM," in *Proc. 2021 CIE Int. Conf. Radar*, Haikou, China, 2021, pp. 2376–2380.

[17] X. Chen and Z. Yang, "Localizing more sources than sensors in presence of coherent sources," in *Proc. 2022 IEEE Int. Conf. Acoust., Speech, Signal Process. (ICASSP)*, Singapore, 2022, pp. 5013–5017.

[18] X. Xu, Z. Ye, Y. Zhang, and C. Chang, "A deflation approach to direction of arrival estimation for symmetric uniform linear array," *IEEE Antennas Wireless Propagat. Lett.*, vol. 5, pp. 486–489, 2006.

[19] S. Qin, Y. D. Zhang, and M. G. Amin, "DOA estimation of mixed coherent and uncorrelated targets exploiting coprime MIMO radar," *Digital Signal Process.*, vol. 61, pp. 26–34, 2017.

[20] Q. Wu, Y. D. Zhang, M. G. Amin, and B. Himed, "Complex multitask bayesian compressive sensing," in *Proc. 2014 IEEE Int. Conf. Acoust., Speech, Signal Process. (ICASSP)*, 2014, pp. 3375–3379.

[21] R. A. Horn and C. R. Johnson, *Matrix Analysis*. Cambridge University Press, 2012.

[22] C.-L. Liu and P. Vaidyanathan, "Remarks on the spatial smoothing step in coarray MUSIC," *IEEE Signal Process. Lett.*, vol. 22, no. 9, pp. 1438–1442, 2015.